NAIC-ID(RS)T-0369-95

NATIONAL AIR INTELLIGENCE CENTER

EXPERIMENT ON A FREE-ELECTRON LASER WITH A TAPERED WIGGLER AND ANALYSIS OF RESULTS

by

Zhao Donghuan, Wang Jian

Approved for public release: distribution unlimited

NAIC-ID(RS)T-0369-95

HUMAN TRANSLATION

NAIC-ID(RS)T-0369-95 2 October 1995

MICROFICHE NR: 95C000609

EXPERIMENT ON A FREE-ELECTRON LASER WITH A TAPERED WIGGLER AND ANALYSIS OF RESULTS

By: Zhao Donghuan, Wang Jian

English pages: 13

Source: Qiangjiguang Yu Zizishu, Vol. 4, Nr. 3, August 1992; pp. 381-386

Country of origin: China
Translated by: Leo Kanner Associates
F33657-88-D-2188
Requester: NAIC/TATD/Dr. James Newton

THIS TRANSLATION IS A RENDITION OF THE ORIGINAL FOREIGN TEXT WITHOUT ANY ANALYTICAL OR EDITORIAL COMMENT STATEMENTS OR THEORIES ADVOCATED OR IMPLIED ARE THOSE OF THE SOURCE AND DO NOT NECESSARILY REFLECT THE POSITION OR OPINION OF THE NATIONAL AIR INTELLIGENCE CENTER.	PREPARED BY: TRANSLATION SERVICES NATIONAL AIR INTELLIGENCE CENTER WPAFB, OHIO

GRAPHICS DISCLAIMER

All figures, graphics, tables, equations, etc. merged into this translation were extracted from the best quality copy available.

EXPERIMENT ON FREE-ELECTRON LASER WITH A TAPERED WIGGLER AND ANALYSIS OF RESULTS

Zhao Donghuan and Wang Jian
Shanghai Institute of Optics and Fine Mechanics,
Chinese Academy of Sciences, Shanghai 201800

ABSTRACT Experiments on a Raman FEL with a tapered field have been done. A maximum radiution output of 31MW at 8 ~ 10.4mm has been obtained with an energy efficiency of 9.68%. The tapering technique is effective in increasing the efficiency in the Raman FEL for large current and low energy electron beam.

KEY WORDS transformation efficiency of energy, tapering wiggler technique.

I. INTRODUCTION

Theory and experiments prove that the Raman free-electron laser [FEL] with a high-current, low-energy relativistic beam is a more ideal apparatus, capable of providing high power and continuous coherent adjustable millimeter and submillimeter wave radiation source [1-6]. Research revealed that a variable-parameter wiggler FEL can also increase the laser output power

[7]. This kind of wiggler apparatus was applied at the Lawrence Livermore National Laboratory (LLNL) in the United States to obtain A 1GW high-power output with an 8mm wavelength [6]. The electron energy conversion efficiency is 34%, thus becoming an experiment with the highest FEL efficiency at present.

The above-mentioned LLNL experiment was based on high-current, medium-energy (3.5MeV) electron beams. However, for high current, low energy (3.45MeV) electron beams, there has no report of adopting the tapered wiggler technique to increase the FEL conversion efficiency.

II. Experimental Principles

The relationship between the FEL coherent radiation wavelength and electron energy is [8]

$$\lambda_s = (\lambda_w / 2\gamma_r^2)[1 + \frac{1}{2}(eB_w\lambda_w / 2\pi mc)^2] \tag{1}$$

λ_s is the coherent radiation wavelength; γ_r is the resonant electron energy factor; and B_W and γ_W are the wiggler field intensity and period, respectively.

After the electron radiation is captured, most electron energy will be lower than the resonant-state energy. To continuously maintain the radiation state of the γ_s operating wavelength, we know from Eq. (1) that in the gradually descending state of γ_r, if the field intensity B_W or the period length λ_W synchronously decrease with decrease of γ_r, then the radiation

status can be continuously maintained.

Thus, the interaction time (or length) between the electron and the wave is prolonged, and the energy conversion efficiency is raised. Therefore, the variable-parameter wiggler can increase the FEL output power.

For an FEL with constant λ_W and tapered reduction of field intensity B_W, its efficiency can be expressed as [9]:

$$\eta_{e1}=f_{e1}\frac{a_w(0)a_s k_s L}{2\gamma_r(\gamma_r-1)}\sin\psi_{r1}\left[\frac{1+a_w(L)/a_w(0)}{2}\right] \qquad (2)$$

In the equation, f_{e1} is the $_e$lectron capture function; L is the effective length of interaction between electrons and waves; k_s is the wave vector of the radiation field; ψ_{r1} is the resonant electron synchronized phase; k_s is the vector potential of the radiation field. $a_W(0)$ and $a_W(L)$ are, respectively:

$$a_w(0)=\frac{eB_w(0)\lambda_w}{2^{3/2}\pi mc}$$
$$a_w(L)=\frac{eB_w(L)\lambda_w}{2^{3/2}\pi mc} \qquad (3)$$

$B_W(0)$ and $B_W(L)$ are, respectively, the field intensities at the beginning and ending terminals of the wiggler apparatus. From Eq. (2), we can obtain the result that the constant wiggler FEL efficiency is:

$$\eta_{e0}=f_{e0}\,\frac{a_w a_s k_s L}{2\gamma_r(\gamma_r-1)}\sin\psi_{r0} \tag{4}$$

It can be seen that the ratio of efficiencies for two types of lasers in the same category is:

$$\frac{\eta_{e1}}{\eta_{e0}} \approx \frac{f_{e1}}{f_{e0}}\left[\frac{1+a_w(L)/a_w(0)}{2}\right]\sin\psi_{r1}/\sin\psi_{r0} \tag{5}$$

Assume that the tapered wiggler mean-field intensity and the constant wiggler field intensity are equal to each other in the experiment, then we have [9]:

$$\frac{f_{e1}}{f_{e0}} \approx \left(\frac{a_w(0)}{a_w(L)}\right)^{1/2} = \left(\frac{B_w(0)}{B_w(L)}\right)^{1/2} \tag{6}$$

To estimate the phase ψ_r, we can use the following relation [7]:

$$F(\psi) = -\Lambda(\cos\psi+\sin\psi_r) \tag{7}$$

In the equation, $\Lambda=\frac{a_w a_s \omega_s}{\gamma_r c}$, when $\psi=\psi_r$, Eq. (7) indicates that there is the mass-force position potential (minimum value) at the radiation state.

It is assumed that the rational tapered parameter synchronously reduces a_w and γ_r, then Λ remains constant; however, with prolonged resonant time, there will be more electron energy converted into radiation energy. Then in the situation of the variable-parameter wiggler, F will decrease further. However, the corresponding resonant-state phase ψ_r will be correspondingly increased. For example, in the constant

wiggler situation, it is assumed that in the resonant-state electron phase, $\psi_{r0}=15^{\circ}$. At this stage, during the radiating state $F(15^{\circ})=-1.0336\Lambda$. After the rational varying parameters, $F(\psi)$ decreases as -1.1278Λ. Then during the varying parameter wiggler state, the electron resonant-state phase $\psi_{r1}=30^{\circ}$. Since in the radiation state $0\leqslant\psi_r\leqslant\frac{\pi}{2}$, this indicates that the electron resonant state phase increases with the increased electron energy thus extracted.

Assume that in the experiment, it is selected that $B_W(L)$ is 45% of $B_W(0)$, and assume $\psi_{r0}=15^{\circ}$ and $\psi_{r1}=35^{\circ}$, then from the above-mentioned equation we can initially estimate $\eta_{e1}/\eta_{e0}=2.395$. It can be seen that even not considering the effect of interaction time, the tapered wiggler FEL efficiency is 2.395 x the efficiency of the constant wiggler FEL efficiency.

By using the tapered wiggler technique to increase the FEL efficiency, the key is how to synchronously reduce the experimental field intensity $B_W(Z)$ and the resonant-state energy factor γ_r. For convenience in analysis, it is defined that the unit length field intensity tapering rate is

$$\delta=\frac{B_W(0)-B_W(z)}{B_W(0)(z-z_0)} \tag{8}$$

By using Eq. (1), we can obtain

$$\delta=\frac{1}{l}\left[1-\left(\frac{4\gamma_r^2-2\mu^2}{4\gamma_0^2-2\mu^2}\right)^{\frac{1}{2}}\right] \tag{9}$$

In the equation, l is the effective interaction distance, $\mu=(\lambda_W/\lambda_s)^{\frac{1}{2}}$. γ_0 is the incident relativistic electron energy

factor. Eq. (9) indicates that the tapering rate is different in selecting different energy-relativistic electrons. However, for the same energy there are different effects for different tapering rates in selecting the relativistic electrons. This is consistent with the numerical simulation results [10].

III. Experimental Layout

For convenience in repairing the experimental results of the constant-parameter wiggler FEL, the experiments were conducted on the high-current (800A), low-energy (0.45MeV) electron beam Raman FEL in the authors' institute. There was some difference that a conical shaped dual-thread undulator replacing the original cylindrical dual-thread undulator, and a 1.56-m long copper shaft waveguide shifter tube to replace the original 1.5-m stainless shifter tube.

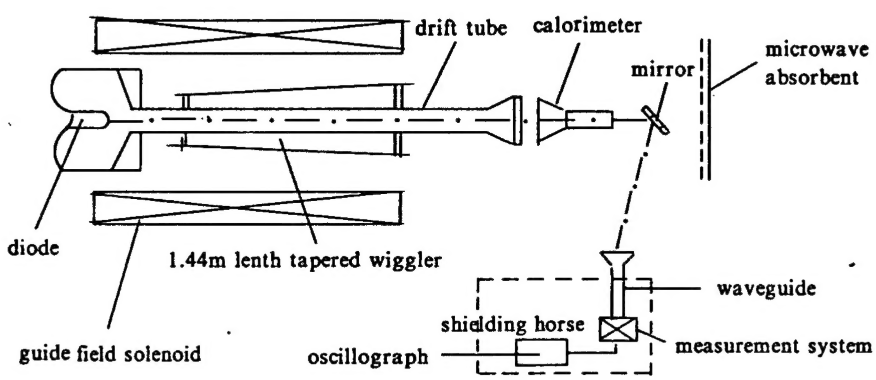

Fig. 1 is the schematic experimental layout. 0.45MeV electrons are generated by a diode without foil. The distance between the diode, anode, and cathode is 8.5mm, and an OD6 hole is opened at the anode center, thus applying the magnetic field

submerged type. The electron beam should be kept sufficiently cold in order to satisfy the velocity scatter along the tapered shaft direction of 1 per mil of Raman scatter, and the radius of the electron beam waist is 3mm.

In the experiment, the guiding magnetic field can be adjusted within the range between 0 and 20kGs; its function is to restrain the axial-direction beam current of the high-current low-energy electron beam generated by the foil-free diode, and to guide so that the electron cyclic motion matches with the wiggler field in the undulator. When guiding the functions of field B_0 and the wiggler field B_W, the relation between the transversely-directed velocity $\mathbf{v}_\perp$ and the longitudinal directed velocity $\mathbf{v}_\parallel$ can be expressed as [11]:

$$\left.\begin{aligned} v_\perp &= \Omega_\perp v_\parallel / (\Omega_0 - \gamma k_W v_\parallel) \\ v_\parallel^2 + v_\perp^2 &= (1-\gamma^{-2})c^2 \end{aligned}\right\} \tag{10}$$

In the equation,

$$\left.\begin{aligned} \Omega_\perp &= eB_W/mc \\ \Omega_0 &= eB_0/mc \end{aligned}\right\} \tag{11}$$

In the interaction zone between electrons and waves, a 1.65-m copper waveguide shifter tube replaces the original 1.5-m stainless steel shifter tube in order to improve the magnetic infiltration effect of the tube walls. The internal and external diameters of the shifter tube is 20 and 23mm.

The 1.44-m dual-spiral tube undulator is wound with the conical shape dual-spiral thread; the conicity of the spiral

surface is 0.3°. With excitation by the reverse-phase current, the central shaft of the dual-spiral thread can form a circular polarized transversely-directed wiggler field of the spiral varying oscillation amplitude [12]. The measured magnetic field cycle and the cycle of dual-spiral thread (λ_W=24mm) are equal to each other. At the central shaft, the ratio of field intensity of $B_w(0)/B_w(L)$ between the beginning terminal and the end terminal is 2.56. In order to let the undulator entrance of the electron beam have a more even transition field, eight high-impedance wires are connected in parallel in the terminal zone of the dual-spiral thread. Fig. 2 gives the distribution profile of the transverse magnetic field along the central axis of the dual

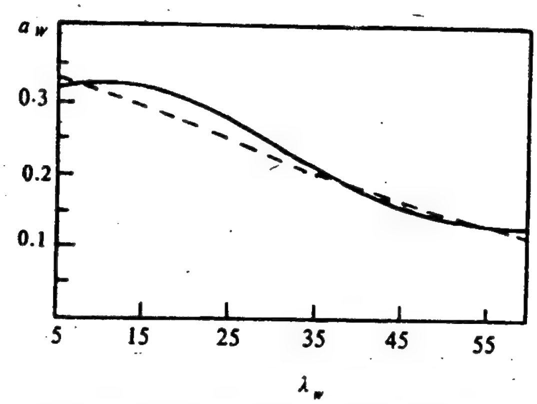

Fig.2 Transversc magnetic field profile of tapered wiggler, Dotted line is the numerical computation and solid line is the measurem ent evaluation.

spiral tube. The dotted curve shows the calculation results of an approximation formula. Since the resistive effect at the side route of the entrance terminal of the undulator, and the effect of current in the wire outside of the wire terminal tube are neglected in the calculation, there is greater error between the

measurement values (solid curves) and the calculated values at both terminals. However, these two are closer at the middle portion.

The coherent radiation of the electron beam is outputted from a conical shaped horn aperture. The energy was measured with a carbon receptacle calorimeter. The radiation waveform enters an 8mm waveguide tube through a reflective lens. The distance from the output of the horn aperture to the waveguide tube after reflection is approximately 4m. After passing through the crystal wave detector, the waveform is acquired with an oscillograph. To prevent interference, all waveform detecting systems are installed in a shielded chamber.

IV. Experimental Results

Since the variable-amplitude wiggler magnetic field is selected as the pumping field, there will be some changes in the operating conditions of the FEL. B_0 of the optimal guiding field and the $B_w(0)$ of the wiggler field are 11.83 and 1.96kGs, respectively. Changes in the guiding field an the wiggler field are obtained by changing the pulsation voltage applied to the guiding field armature and the undulator dual-spiral armature. Table 1 lists a set of better experimental data. U_g and U_w are the values of the pulsating voltage applied to the armatures of the guiding field and the wiggler field. From Table 1, there are great variations in the output coherent radiation energy under different guiding fields.

The optimal operating points of the experiments are determined in two steps. First, a guiding field is selected to change the measured variation in radiation energy of the wiggler field intensity (Fig. 3). From Fig. 3, determine the optimal wiggler field intensity. Then change the guiding field and measure the energy variation. Finally, the guiding field

Table 1 Measurement emittance energy guide vs. magnetic field

U_g/V	B_0/Gs	U_W/V	$B_W(0)$/kGs	Calorimeter	E/mJ
500	3.46	1350	1.96	2	10.12
800	5.53	1350	1.96	16	80.96
900	6.22	1350	1.96	38	192.28
1000	6.92	1350	1.96	21	106.26
1100	7.61	1350	1.96	52	263.12
1200	8.30	1350	1.96	6	30.36
1300	8.99	1350	1.96	109	551.54
1400	9.69	1350	1.96	83	419.98
1500	10.38	1350	1.96	21	106.26
1600	11.07	1350	1.96	57	288.42
1700	11.83	1350	1.96	132	667.92
1800	12.45	1350	1.96	76	384.56
1900	13.15	1350	1.96	116	586.96
2000	13.90	1350	1.96	70	354.42

corresponding to the maximum radiation state is the optimal field intensity of the operating point.

Fig. 4 shows the corresponding curves of the optimal wiggler field coherent radiation energy varying with the guiding field. Solid curves in the figure represent the results of the tapered wiggler; the dotted curves represent the results of the constant wiggler [13]. Comparing the results of both experiments, we can clearly see that the radiation energy of the tapered wiggler is much greater than that of the constant wiggler FEL.

In addition, the varying-parameter wiggler has a greater improvement in the selecting range of the guiding field than the constant-parameter wiggler. After the radiation energy of the varying-parameter wiggler arrives at the maximum value, there is a higher local peak value with increase in guiding field intensity. However, after the output radiation energy of the constant-parameter wiggler reaches the maximum, the energy

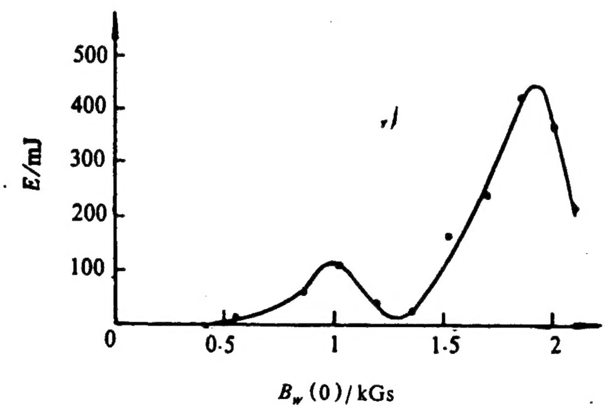

Fig. 3 Guide magnetic field B_0 is 12.4KG the relative curve between emittance energy wiggler magnetic field $Bw(0)$.

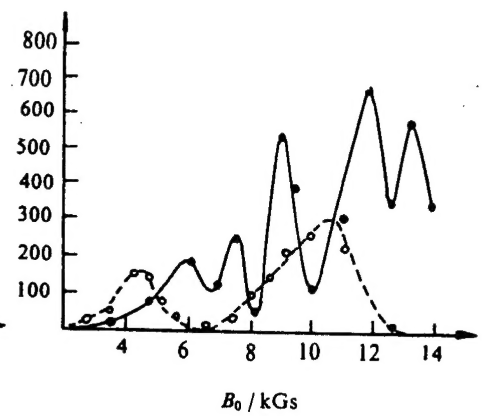

Fig. 4 Relativce curves between the output energy of emittance and guide magnetic field under the optimum wiggler.
Result of tapereing wiggler (solid line) result of constant (dot line).

rapidly decreases and approaches zero, with increase in the guiding field intensity. This is so because the FEL electron beam of the tapered wiggler field has a wider range $B_w(0) \sim B_w(L)$ under the action of field intensity. Therefore, the matched guiding field also has a corresponding range. Thus, it is difficult to implement the constant wiggler FEL.

Fig. 5 shows the coherent radiation waveforms for three different guiding fields. They indicate that there exists a

local radiation energy peak with varying B_0 of the guiding field. This again indicates that the varying-parameter wiggler FEL has a wider range for selecting the guiding field.

When selecting the optimal operating conditions, the radiation energy measured with a carbon-receptacle calorimeter is 668mJ. The radiation wavelength range is approximately 8 to 10.4mm; the output peak power was 31MW; the diode voltage is 0.4MV, and the electron beam peak current is about 800A. This

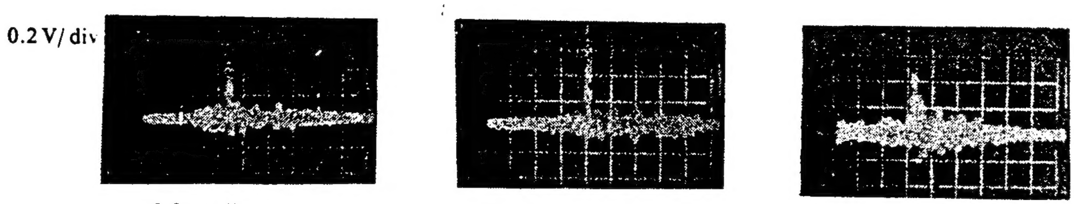

0.2ns/div a. 8.98kGs引导场　0.2ns/div b. 11.83kGs 引导场　0.2 ns/div c. 13.29 kGs 引导场

Fig. 5 When $B_W(0)$ is 1.98KG the photographic waveforms of laser relative to different guide magnetic fields.
a. 8.98KG magnetic field. b. 11.83KG guide magnetic field. c. 13.29KG guide magnetic field.

indicates that the electron beam input power is 300MW. Then we obtain the result that the electron energy conversion efficiency is 9.68%. However, for the 1.5-m constant wiggler Raman FEL, its efficiency is 3.7% [13]. This indicates that the laser energy is upgraded by 2.64-fold by using the tapered wiggler technique. Hence, the adoption of the tapered wiggler technique to increase the Raman FEL efficiency of high-current, low-energy (0.4MeV) electron beams is still effective.

The authors are grateful to all colleagues of team 101 of the Shanghai Institute for providing necessary equipment in the

overall experiment.

The first draft of the article was received on September 27, 1991; the final revised draft was received for publication on December 28, 1991.

REFERENCES

[1] Kroll NM and Mcmullin WA. *Phys Rev A*, 1978, **17**:300 ~ 308.
[2] Bernstein IB and Friedleand L. *Phys Rev A*, 1981, **23**:816 ~ 823.
[3] Shiozawa TJ. *Appl phys*, 1983, **54**:3712 ~ 3722.
[4] Birkett DS et al. *IEEE J Quan elec*, 1981, QE-**17**: 1348 ~ 1353.
[5] Pasour JA and Gole S H. *IEEE J Quan Elec*, 1985, QE-**21**: 845 ~ 859.
[6] Qrzechowski TJ et al. *Phys Rev Lett*. 1996, **57**:2172 ~ 2175.
[7] Kroll NM et al. *IEEE J Quan Elec*, 1981, QE-**17**: 1436 ~ 1468.
[8] Slater JM. *IEEE J Quan Elec*. 1981, QE-**17**: 1476 ~ 1479.
[9] Bhowmik A et al. *IEEE J Quan Elec*, 1985, QE-**21**: 998 ~ 1006.
[10] 田世洪等，强激光与粒子束，1990, **2** (4):467 ~ 473.
[11] Freand HP et al. *IEEE J Quan Elec*, 1985, QE-**21**: 1081 ~ 1082.
[12] 赵东焕．中国激光，1988, **15** (10):620 ~ 622.
[13] 陆载通等．光学学报，1989, **9** (9):780 ~ 786.

DISTRIBUTION LIST

DISTRIBUTION DIRECT TO RECIPIENT

ORGANIZATION	MICROFICHE
B085 DIA/RTS-2FI	1
C509 BALLOC509 BALLISTIC RES LAB	1
C510 R&T LABS/AVEADCOM	1
C513 ARRADCOM	1
C535 AVRADCOM/TSARCOM	1
C539 TRASANA	1
Q592 FSTC	4
Q619 MSIC REDSTONE	1
Q008 NTIC	1
Q043 AFMIC-IS	1
E404 AEDC/DOF	1
E410 AFDTC/IN	1
E429 SD/IND	1
P005 DOE/ISA/DDI	1
1051 AFIT/LDE	1
P090 NSA/CDB	1

Microfiche Nbr: FTD95C000609
NAIC-ID(RS)T-0369-95